Proceedings of the 13th
IEEE International Conference on Nanotechnology
Beijing, China, August 5-8, 2013

# A Molecular Dynamics Study about Two Way Tuning of Thermal Conductivity in Graphene: Strain and Doping *

Chengjian Li[1], Gang Li[2] and Huijuan Zhao[3]

***Abstract*— Thermal conductivity becomes an important material property measure in MEMS/NEMS applications. Recently, graphene has been proved to have superior thermal conductivity, which brought tremendous potential for nanoscale thermal transport management applications. In this study, we adopt the molecular dynamics simulation method to investigate the thermal conductivity variation of graphene with respect to chirality, strain, hydrogen doping and the deformation of the structure. We investigate thermal conductivity variation and various deformation modes of graphene under single-side patterned hydrogenation stripes. We show that graphene thermal conductivity can be tuned by deformation modes and hydrogenation doping density.**

## I. INTRODUCTION

Graphene has attracted researchers' attention in the last decade since it was first observed experimentally [1]. As a stable two dimensional honeycomb lattice of carbon atoms, graphene has excellent mechanical [2], [3] and electronic properties [4], [5], as well as an ultra-high thermal conductivity [6], [7]. Since power dissipation and heat removal become a critical issue in the development of next generation integrated circuits and electronics, graphene becomes a desirable material for electronic and thermal management devices [8]. As the material properties of graphene vary with the size [9], geometry [10], strain [11], doping [12], defects [13], [14] and other factors, it is important to investigate thermal conductivity variations with these factors in order to meet the application requirement and achieve optimal control of the thermal conductivity of graphene.

With the Fourier's law, thermal conductivity can be defined as $\kappa = -q/\nabla T$, where $q$ is the heat flux and $\nabla T$ is the temperature gradient. In solid crystal, heat are generally conducted by electrons and phonons, i.e. $\kappa = \kappa_e + \kappa_p$, where $\kappa_e$ and $\kappa_p$ are the electron and phonon contributions, respectively. In most metal materials, $\kappa_e$ is dominant due to the large concentration of the free carriers. In carbon materials, such as graphene, $\kappa_p$ is dominant due to the strong covalent $sp^2$ bonding between carbon atoms. In nanoscale, $\kappa_p$ is closely related to size, boundary conditions and geometry of the atomistic structures due to the ballistic transport of phonons and significant or even dominant phone-boundary scattering. Numerical simulations have been conducted to show that thermal conductivity of graphene has significant size dependence and increases dramatically with the increasing length along the heat conduction direction [15], [16]. The thermal conductivity of graphene nanoribbon decreases remarkably under tensile strain [17], [18]. The hydrogenation of graphene will also bring a rapid drop of the graphene's thermal conductivity [19], [20]. However, to the authors' knowledge, no systematical study has been conducted to investigate the deformation modes of graphene under compressive strain with/without doping and the corresponding thermal conductivity variation.

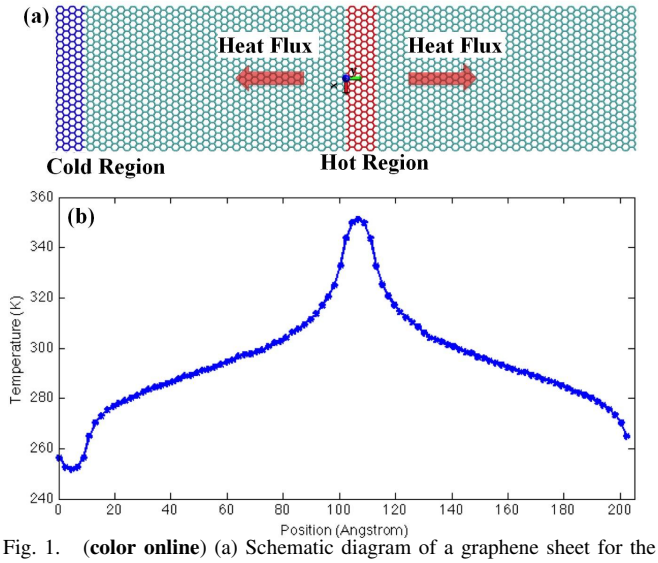


Fig. 1. (**color online**) (a) Schematic diagram of a graphene sheet for the calculation of thermal conductivity. With periodic boundary condition in in-plane directions, the graphene sheet has one cold region (blue), two heat flux regions (green) and one hot region (red); (b) A sample temperature profile with non-equilibrium steady state after heat flux has been imposed. The thermal conductivity can then be calculated using the slope of the temperature in the heat flux region.

In this study, we performe non-equilibrium molecular dynamics simulation to investigate the thermal conductivity variation of graphene with the control of strain and doping fraction. It is observed that the thermal conductivity of graphene decreases more than 40% with a 10% tensile strain. With hydrogen doping, the thermal conductivity drops dramatically first and then decrease slowly with the increasing of the hydrogen doping fraction. With different hydrogen doping patterns, we identify different deformation modes due to the local stress caused by H-C bonding. In the following sections, we first introduce the method to calculate thermal conductivity and molecular dynamics set up. Next we discuss the results and findings. The conclusions are presented at the end.

*This work was supported from Clemson startup fund and National Science Foundation

[1]Chengjian Li is Ph.D. candidate of Mechanical Engineering, Clemson University, Clemson, SC, 29634, USA

[2]Gang Li is associate professor of Mechanical Engineering, Clemson University, Clemson, SC, 29634, USA

[3]Huijuan Zhao is assistant professor of Mechanical Engineering, Clemson University, Clemson, SC, 29634, USA hzhao2 at clemson.edu

## II. METHOD

Non-equilibrium molecular dynamics simulations are performed using LAMMPS [22] with the adaptive intermolecular reactive empirical bond order (AIREBO) potential to describe C-C, C-H interactions [21]. AIREBO potential has been shown to accurately capture the thermal and mechanical properties of graphene [13], [17] as well as the bonding between carbon and hydrogen atoms. The cutoff parameter of C-C interaction is set to be 2.0Å in order to avoid the nonphysical results near the fracture region during the unaxial tension test. The H-H interaction is not considered in this study. The graphene sheet is decomposed into cold, hot, and heat flux regions as shown in Fig. 1(a). The length of both cold and hot regions is equal to 5% of the graphene sheet length. The length of the heat flux region is 45% of the graphene sheet length. Periodic boundary condition is applied in the longitudinal and transverse directions of the graphene. A 5nm thick vacuum space is applied on both sides of the graphene sheet to prevent the non-bonding long range interaction along the direction which is perpendicular to the graphene sheet . The graphene sheet is first relaxed to the equilibrium state at 300K for at least 50ps under the NPT ensemble. The time step is set to be 0.5fs. Next, the NVE ensemble is applied and the heat flux is imposed on the system by exchanging the velocity of the atom with the highest kinetic energy in the hot region with the velocity of the atom with the lowest kinetic energy in the cold region. Over $t_s = 100$ps, the non-equilibrium steady state can be reached from the exchanging process. A stable temperature gradient is induced into the system. Along the heat flux direction, we divided the graphene sheet into bins with the width of $1.5a$, where $a = 1.42$Å is the lattice constant. The temperature profile (shown in Fig.1(b)) after reaching the non-equilibrium steady state is calculated by averaging the temperature of each bin as,

$$T_i = \frac{1}{3N_i k_B} \sum_{j=1}^{N_i} m v_j^2, \tag{1}$$

where, $T_i$ is the temperature of $i$th bin, $N_i$ is the number of carbon atoms in $i$th bin, $k_B$ is Boltzmann's constant, $m$ is the mass of carbon atom and $v_j$ is the velocity of atom $j$. Meanwhile, the heat flux $q$ is defined as

$$q = \frac{\Delta E}{2At_s}, \tag{2}$$

where $A$ is the area of heat flux region, $\Delta E$ is the total swap energy given by LAMMPS and $t_s$ is the time for energy swap in the steady state. Thus, the thermal conductivity can be calculated along the heat flux direction from the Fourier law as

$$\kappa = -\frac{q}{\nabla T}. \tag{3}$$

## III. RESULTS AND DISCUSSION

With the method described in the previous section, we first study the thermal conductivity variation with the length of the heat flux region. As shown in Fig. 2(a), thermal conductivity increases significantly with the increasing of the length of heat flux region. Perpendicular to the heat flux direction, the width of graphene sheet is set to be 8.6nm, which has been proved to have no effect to the thermal conductivity of the material. However, the length of the heat conductivity region plays an important role to determine the maximum phonon wavelength the system can carry during the simulation with the periodic boundary condition. The increasing trend of the thermal conductivity matches well with the previous research finding [15].

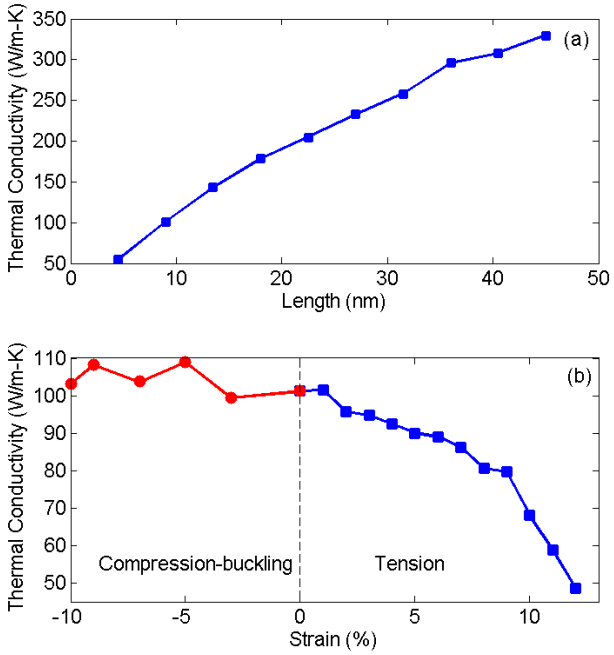


Fig. 2. (**color online**) (a) Thermal conductivity variation with respect to the length of the heat flux region of the graphene sheet. The width of the graphene sheet is fixed at 8.6nm; (b) Thermal conductivity variation with repsect to the strain along the heat flux direction.

Next we investigate the strain effect on the thermal conductivity. We take the graphene sheet with a size of 20.42nm in the length (heat flux) direction and 8.6nm in the width direction. Each of the heat flux region has a length of 9.2nm. Mechanical strain is applied to the graphene sheet with the displacement control method by applying the strain rate $0.001/$ps along the heat flux direction. The NPT ensemble is applied to relax the graphene sheet in the other directions in order to achieve uniaxial tension/compression. Under tensile strain, the graphene sheet is stretched along the heat flux direction. Under compressive strain, the graphene sheet buckles. We define the strain as $(L-L_0)/L_0$ where $L$ is the deformed length of the simulation box in heat flux direction and $L_0$ is the initial length correspondingly. Figure 2(b) shows the thermal conductivity of graphene sheet under strain along the heat flux direction. It clearly shows that the thermal conductivity decreases significantly with the increasing of tensile strain. The thermal conductivity drops around 10% with 5% of the uniaxial tensile strain, but 50% with the 12% of uniaxial tensile strain. However, the variation of thermal conductivity with a compressed

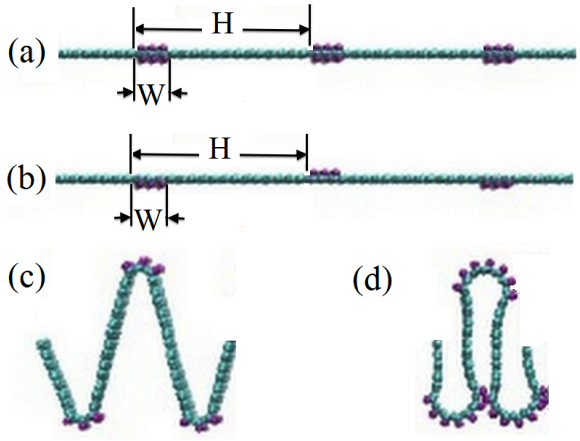


Fig. 3. (**color online**) (a) Initial configuration of graphene sheet with double-sided hydrogenation stripes; (b) Initial configuration of graphene sheet with single-sided hydrogenation stripes alternatively on the two sides; (c) Single sided hydrogenation stripes with $W:H=18.75\%$: relaxed structure of triangular shape (TRI); (d) Single sided hydrogenation stripes with $W:H=37.5\%$: relaxed structure of compact shape (COM).

graphene sheet is very limited.

We next investigate the doping effect on the thermal conductivity. Hydrogen atoms can be doped as single-sided patterned stripes and double-sided patterned stripes respectively, as shown in Fig. 3(a,b). A stripe is defined as the minimum periodic length $H$ including a hydrogenation region with the length of $W$. The doping fraction is defined as ratio of $W:H$. In this study, the graphene sheet size is 20.42nm $\times$8.60nm with the periodic boundary condition along the two in-plane directions. Firstly, we apply a two double-sided hydrogenation stripes along the longitudinal direction (heat flux direction) with $H=4.30$nm and the transverse direction with $H=10.21$nm, respectively. In Fig. 4, it is shown that with the hydrogen doping, the thermal conductivity of graphene sheet drops at least 70%. When the graphene is fully doped with hydrogen atoms on both sides, the thermal conductivity drops 90%, compared to the thermal conductivity of the pristine graphene sheet. It is because the $sp^3$ C-H bonding has weak thermal conductivity than then $sp^2$ C-C bonding. The chirality effect is not significant in this study.

With double-sided patterned hydrogen doping, the relaxed graphene structure remains flat with ripples caused by the local stress from carbon and hydrogen bonding on both sides of graphene in the doping regions. With single-sided patterned hydrogenation stripes, the relaxed graphene structure can not remain planar due to the local stress concentration on one side of the graphene in the hydrogenation regions. We use a graphene sheet of 20.42nm$\times$5.16nm with periodic boundary condition along the in-plane directions. We observed that with different ratio of $W:H$, the doped graphene sheet relaxes to different deformation modes shown in Fig. 3. The relaxed structure with a $W:H=18.75\%$ has the deformation mode of triangular shape (TRI) with a deformed hydrogenation region and a planar graphene region. The relaxed structure with $W:H=37.5\%$ ratio has deformation mode of a compact shape (COM) with a deformed hydrogenation

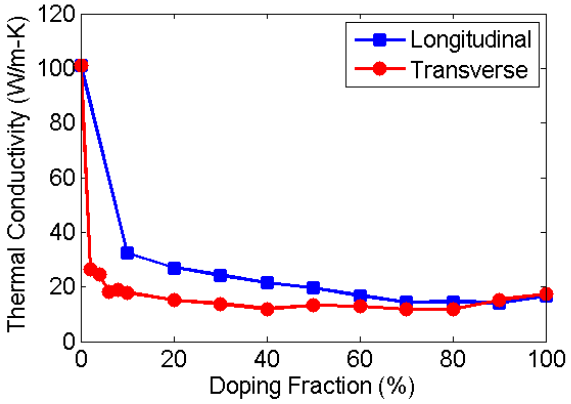


Fig. 4. (**color online**) Thermal conductivity variation with respect to the hydrogen doping coverage both in longitudinal direction (heat flux direction) and in transverse direction (perpendicular to heat flux direction). The grapheen sheet is 204.19Å in length and 85.96Å in width

TABLE I

THERMAL CONDUCTIVITY VARIATION WITH DOPING FRACTION UNDER RELAXED AND UN-RELAXED CONFIGURATIONS.

| W (Å) | doping fraction W/H | Relaxed Structure $\kappa$ (W/m-K)(shape) | Fixed Structure $\kappa$ (W/m-K) |
|---|---|---|---|
| 2.13 | 10.4% | 15.43 (TRI) | 18.58 |
| 4.25 | 20.9% | 9.38 (TRI) | 13.51 |
| 6.38 | 31.32% | 6.93 (TRI) | 10.88 |
| 8.51 | 41.72% | 5.75 (COM) | 10.10 |
| 10.64 | 52.16% | 6.37 (COM) | 8.67 |
| 12.76 | 62.55% | 7.84 (COM) | 8.42 |
| 14.89 | 72.99% | 10.32 (COM) | 8.47 |
| 17.02 | 83.33% | 10.16 (COM) | 8.15 |
| 19.14 | 93.83% | 12.02 (COM) | 7.89 |

region and a non-planar graphene region. In table I, we consider the 20.4nm$\times$5.16nm periodic graphene with 10 stripes along the transverse direction, which means for each stripe $H$ is 2.04nm. By using the same technique described in the previous section, we calculate the thermal conductivity of both the fixed graphene sheet (remain planar) and the relaxed graphene sheet with different deformation modes. The fixed graphene sheet shows a decreasing trend with the increasing width of $W$. For the relaxed graphene structure, we found that the thermal conductivity decreases faster with TRI mode than with the fixed graphene sheet. Moreover, the COM mode changes the trend of thermal conductivity from monotonically decreasing to slightly increasing. The results show that the thermal conductivity can be tuned by adjusting the doping fraction, stripe width and the deformation modes.

## IV. CONCLUSION

In this study we adopt molecular dynamics simulation technique to investigate the thermal conductivity of graphene sheet under different length, strain and doping fraction. We demonstrate that the thermal conductivity of graphene sheet increases with the increasing length of heat flux region. The hydrogen doping brings a significant drop to the thermal conductivity. More importantly, single-side patterned hydrogenation can lead the graphene sheet to various deformation

modes which can influence the trend of thermal conductivity variation.

## V. ACKNOWLEDGMENT

We gratefully acknowledge support from Clemson startup fund and National Science Foundation support under Grant number CBET-0955096.

## REFERENCES

[1] K. S. Novoselov, A. K. Geim, S. V. Morozov, D. Jiang, Y. Zhang, S. V. Dubonos, I. V. Grigorieva and A. A. Firsov, Electric Field Effect in Atomically Thin Carbon Films, Science, vol 306, pp 666-669, Oct. 2004.

[2] C. Lee, X. Wei, J. W. Kysar, and J. Hone, Measurement of the Elastic Properties and Intrinsic Strength of Monolayer Graphene, Science, vol 321, pp 385, Jul. 2008.

[3] C. Gomez-Navarro, M. Burghard, and K. Kern, Elastic Properties of Chemically Derived Single Graphene Sheets, Nano letters, vol 8, pp 2045, Jun 2008.

[4] K. S. Novoselov, A. K. Geim, S. V. Morozov, D. Jiang, M. I. Katsnelson, I. V. Grigorieva, S. V. Dubonos, and A. A. Firsov, Two-dimensional gas of massless Dirac fermions in graphene, Nature, vol 438, 197-200, Nov. 2005.

[5] Y. Zhang, Y. Tan, H. L. Stormer and P. Kim, Experimental observation of the quantum Hall effect and Berry′s phase in graphene, Nature, vol 438, pp 201-204, Nov. 2005.

[6] A.A. Balandin, S. Ghosh , W. Bao , I. Calizo , D. Teweldebrhan , F. Miao , C. N. Lau, Superior Thermal Conductivity of Single-Layer Graphene, Nano Letters, vol 8, pp 902-907, Feb. 2008.

[7] S. Ghosh, I. Calizo, D. Teweldebrhan, E. P. Pokatilov, D. L. Nika, A. A. Balandin, W. Bao, F. Miao, and C. N. Lau, Extremely high thermal conductivity of graphene: Prospects for thermal management applications in nanoelectronic circuits, Applied Physics Letters, vol 92, 151911, Apr. 2008.

[8] K. Kordas, G. Toth, P. Moilanen, M. Kumpumaki, J. Vahakangas, A. Uusimaki, R. Vajtai and P M Ajayan, Chip cooling with integrated carbon nanotube microfin architectures, Applied Physics Letters, vol 90, pp 123105, Mar. 2007

[9] H. Zhao, K. Min and N. R. Aluru, Size and chirality dependent elastic properties of graphene nanoribbons under uniaxial tension, Nano Letters, vol 9, pp 3012-3015, Jul. 2009.

[10] Jiuning Hu, Xiulin Ruan, and Yong P. Chen, Thermal Conductivity and Thermal Recti?cation in Graphene Nanoribbons: A Molecular Dynamics Study, Nano Letters, vol 9, pp 2730-2735, May 2009.

[11] X. Li, K. Maute, M.L. Dunn, and R. Yang, Strain effects on the thermal conductivity of nanostructures, Physical Review B, vol 81, pp 245318, Jun. 2010.

[12] B. Mortazavi, A. Rajabpour, S. Ahzi, Y. Re ?mond, and S.M.V. Allaei, Nitrogen doping and curvature effects on thermal conductivity of graphene: A non-equilibrium molecular dynamics study, Solid State Communication, vol 152, pp 261-264, Feb. 2012.

[13] H. Zhao and N. R. Aluru, Temperature and strain-rate dependent fracture strength of graphene", Journal of Applied Physics, vol 108, pp 1064321, Sep. 2010.

[14] F. Hao, D. Fang, and Z. Xu, Mechanical and thermal transport properties of graphene with defects, Applied Physics Letters, vol 99, pp 041901, July 2011.

[15] D. Wei, Y Song and F. Wang, A simple molecular mechanics potential for ?m scale graphene simulations from the adaptive force matching method, Journal of Chemical Physics, vol 134, pp 184704, May 2011.

[16] A. Cao, Molecular dynamics simulation study on heat transport in monolayer graphene sheet with various geometries, Journal of Applied Physics, vol 111, pp 083528, Apr. 2012.

[17] N. Wei, L. Xu, H. Wang, and J. Zheng, et al, Strain engineering of thermal conductivity in graphene sheets and nanoribbons: a demonstration of magic flexibility, Nanotechnology, vol 22, pp 105705, Mar. 2011.

[18] Z. Guo, D Zhang, and X Gong, Thermal conductivity of graphene nanoribbons, Applied Physics Letters, vol 95, page 163103, Oct 2009.

[19] Q. Pei, Z Sha, and Y. Zhang, A theoretical analysis of the thermal conductivity of hydrogenated graphene, Carbon, vol 49, pp 4752, 2011.

[20] S. Chien, Y. Yang, and C. Chen, Influence of hydrogen functionalization on thermal conductivity of graphene: Nonequilibrium molecular dynamics simulations, Applied Physics Letters, vol 98(3), pp 033107, Jan 2011.

[21] D. W. Brenner, O. A. Shenderova, J. A. Harrison, S. J. Stuart, B. Ni and S. B Sinnott, A second-generation reactive empirical bond order (REBO) potential energy expression for hydrocarbons, Journal of Physics: Condensed Matter vol 14, pp 783 Jan 2002.

[22] S. Plimpton, Fast Parallel Algorithms for Short-Range Molecular Dynamics, Journal of Computational Physics, vol 117, pp 1-19, March 1995.